



Influence of selected plane on the evaluation of tibial tunnel locations using a three-dimensional bone model in double-bundle anterior cruciate ligament reconstruction

Yamamoto, Tetsuya ; Nagai, Kanto ; Araki, Daisuke ; Miyaji, Nobuaki ; Nakanishi, Yuta ; Hoshino, Yuichi ; Kanzaki, Noriyuki ; Matsumoto,...

(Citation)

The Knee, 29:298-304

(Issue Date)

2021-03

(Resource Type)

journal article

(Version)

Accepted Manuscript

(Rights)

© 2021 Elsevier B.V.

This manuscript version is made available under the CC-BY-NC-ND 4.0 license

<http://creativecommons.org/licenses/by-nc-nd/4.0/>

(URL)

<https://hdl.handle.net/20.500.14094/90008440>



1 **Influence of Selected Plane on the Evaluation of Tibial Tunnel Locations Using a Three-**
2 **dimensional Bone Model in Double-Bundle Anterior Cruciate Ligament Reconstruction**

3
4 Tetsuya Yamamoto¹, Kanto Nagai¹, Daisuke Araki¹, Nobuaki Miyaji¹, Yuta Nakanishi¹,
5 Yuichi Hoshino¹, Noriyuki Kanzaki¹, Tomoyuki Matsumoto¹, Takahiro Niikura¹,
6 Ryosuke Kuroda¹, Takehiko Matsushita¹

7 ¹ Department of Orthopaedic Surgery, Kobe University Graduate School of Medicine, Kobe, Japan

8
9 **Corresponding author**

- 10 • Name: Kanto Nagai, MD, PhD
- 11 • Institutional address:
- 12 Department of Orthopaedic Surgery, Kobe University Graduate School of Medicine,
- 13 7-5-1, Kusunoki-cho, Chuo-ku, Kobe, Hyogo, 650-0017, Japan
- 14 • Phone: +81-78-382-5985
- 15 • Email: nagaik@med.kobe-u.ac.jp

16 **1. Introduction**

17 Anterior cruciate ligament (ACL) injury is very common in professional athletes and in people who
18 practice sports regularly. ACL reconstruction (ACLR) aims to eliminate knee instability and prevent post-
19 traumatic osteoarthritis[1,2]. Precise assessment of tunnel locations following anterior cruciate ligament
20 reconstruction (ACLR) is of great importance as tunnel locations have been shown to affect clinical
21 outcomes[3,4]. Few studies in the literature which focus primarily on the clinical outcomes of the tibial
22 tunnel position in ACL reconstruction, however the literatures suggest that more anatomical placement of
23 tibial tunnels confers better stability to the knee and some benefit in terms of functional outcomes[5,6].
24 With respect to the evaluation of tibial tunnel location, a plain lateral radiograph has been originally used
25 to assess the anterior-posterior (AP) location of the tibial tunnel[7–9]. Using a plain lateral radiograph, the
26 center of the tibial insertion point of the ACL was defined as a point along the line parallel to the medial
27 tibial plateau[7] or as a point along the line perpendicular to the tibial axis[10]. In recent years, three-
28 dimensional computed tomography (3DCT) has been used to evaluate the tibial bone tunnel location using
29 a grid method[11–17]. However, the evaluated planes vary among the previous studies[11–17] and there
30 is a concern that tibial tunnel locations may be altered if the selected plane changes. Thus, a unified reliable
31 plane is ideal to discuss and compare the tunnel locations among different surgeons and institutions.

32 There would be two possible planes for tibial tunnel assessments using a grid method with 3DCT; the
33 plane for tibial tunnel aperture evaluation can be the plane which is parallel to the tibial plateau surface
34 (plane A), or the plane which is perpendicular to the tibial shaft axis (plane B). Although sagittal cutting
35 plane of the femur has been shown to affect evaluation of femoral tunnel locations[18], it still remains
36 unknown how the selected plane affects the evaluation of tibial tunnel locations. Therefore, the purpose
37 of the present study was to investigate the influence of a selected plane on the evaluation of tibial tunnel
38 locations using 3DCT, and to compare the locations of the tibial tunnel apertures between the plane A and
39 B after double-bundle ACLR. The hypothesis was that the results of the tibial tunnel locations would be
40 different between plane A and B.

41

42 **2. Materials and methods**

43 This study was a retrospective study of prospectively collected data. Consecutive 34 knees of 34 patients
44 (Age at surgery: 26.8 ± 12.4 years, 17 males and 17 females) who underwent anatomic double-bundle
45 ACLR using hamstring tendon autograft in 2015, were included in this study. The inclusion criteria were
46 (1) unilateral ACL injury diagnosed by clinical examination and magnetic resonance imaging, (2) absence
47 of previous knee surgery, and (3) absence of ligament injury to the contralateral knee.

48

49 **Surgical procedure of anatomic double-bundle ACLR**

50 Anatomic double-bundle ACLR using hamstring tendon autograft was performed by experienced senior
51 surgeons as previously reported[19,20]. The original insertion sites of anteromedial bundle (AMB) and
52 posterolateral bundle (PLB) were identified by using anatomical landmarks arthroscopically. The tibial
53 bone tunnels were created by using the tibial drill guide, and the femoral bone tunnels were created by the
54 transportal technique. The tibial drill guide was adjusted to 45° for PLB and 55° for AMB. The grafts
55 were fixed with a suspensory button for the femur, and a cancellous post screw with a washer for tibial
56 side. Tibial fixation was performed at 0° for the PLB and at 30° of knee flexion for the AMB with manual
57 maximum power.

58

59 **Data processing**

60 Two weeks following the surgery, 3DCT images (Aquilion 64, Toshiba Medical Systems, Otawara, Japan)
61 were taken for all knees, with a slice spacing of 0.5mm and a resolution of 512×512 pixels per image[18].
62 Bone tunnel of the tibial region was extracted via a manual method using Mimics® (Materialise, Leuven,
63 Belgium). 3D bone models of the proximal tibia were also created. Tibial bone tunnel regions were
64 obtained by a region growing function in the segmentation software on each computed tomography slice

65 to obtain a 3D tunnel volume. These data were transferred to a 3D modeling software software 3-matic®
66 (Materialise) in order to create planes A and B.

67 Plane A, which is parallel to the tibial plateau surface, was obtained by painting medial and lateral tibial
68 articular surfaces with the function of “wave brush mask” (**Figure 1**). Plane B, which is perpendicular to
69 the proximal tibial shaft axis, was obtained as follows (**Figure 2**). Briefly, the proximal tibial shaft was
70 selected with 10cm width using the function of “wave brush mask”. The best-fit cylinder of the selected
71 proximal tibia was automatically created, and the axis of the proximal tibial shaft was obtained. Eventually,
72 plane B was determined. In the proximal-distal direction, both plane A and B was put beneath the aperture
73 of the tibial tunnels where a complete ellipse could be drawn around the tunnels. Additionally, the
74 difference in coronal alignment was evaluated between planes A and B (°).

75

76 **Evaluation of the locations of tibial tunnel apertures**

77 Locations of the tibial tunnel apertures were evaluated according to the previously reported
78 methods[15,21]. In short, the AP and medial-lateral (ML) edges of the proximal tibial plateau were
79 identified using identifiable landmarks and these points were used to create a grid system on planes A and
80 B, respectively. Each center of the tunnel aperture was then identified within the grid system. Finally, the
81 location was expressed as a percentage of tibial plateau anterior to posterior depth and medial to lateral
82 width using ImageJ (National Institutes of Health, Bethesda, Maryland) (**Figure 3**). The dimensions of
83 the tibial tunnel apertures were also assessed using ImageJ. The diameter (mm) of the major and minor
84 axes of the ellipse were measured in each plane.

85 To evaluate intra-observer and inter-observer reproducibility of measurements obtained by the ImageJ
86 software, all measurements were performed twice by the same surgeon with more than 2 weeks interval,
87 and another examiner measured once to assess inter-rater repeatability. Intraclass correlation coefficients
88 (ICC) for intra-observer were 0.92 and 0.90 for AMB and PLB in plane A, and 0.93 and 0.95 for AMB

89 and PLB in plane B, respectively. Inter-observer ICC were 0.91 and 0.91 for AMB and PLB in plane A,
90 and 0.92 and 0.94 for AMB and PLB in plane B, respectively.

91 The study protocol was approved by the Institutional Review Board of our institution (ID No. B190055),
92 and written informed consent was obtained from all patients before their enrollment.

93

94 **Statistical Analysis**

95 A priori power analysis using G power 3.1 (Christian Albrecht University, Kiel, Germany) indicated that
96 a sample size of at least 17 patients per group was necessary to detect an intergroup difference of 0.1%,
97 in each parameter with effect size of 0.8, an alpha of 0.05 and a power of 80%. A paired t-test was used
98 to compare the data obtained from planes A and B. For all analyses, statistical significance was set at $P <$
99 0.05. All data were reported as mean \pm standard deviation (SD).

100

101 **3. Results**

102 On plane A, the locations of the AMB and PLB tibial tunnel apertures were $36.1 \pm 7.1\%$, $50.6 \pm 6.3\%$ in
103 the AP direction, and $45.0 \pm 2.2\%$, $45.5 \pm 1.8\%$ in the ML direction, respectively. On plane B, the locations
104 of the AMB and PLB tibial tunnel apertures were $38.5 \pm 6.3\%$, $52.9 \pm 5.7\%$ in the AP direction, and 43.5
105 $\pm 2.1\%$, $43.9 \pm 1.5\%$ in the ML direction, respectively. AMB and PLB tunnel apertures in plane A were
106 significantly more laterally located than in plane B (**Figure 4**, AMB; $P = .0021$, PLB; $P = .0006$). Mean
107 differences in the ML direction were 1.5% (95% confidential interval [CI]; 0.5-2.6) in AMB, and 1.7%
108 (95% CI; 0.8-2.5) in PLB. On the other hand, there were no significant differences in AMB and PLB
109 tunnel locations in the AP direction between planes A and B (**Figure 4**). Mean differences in the AP
110 direction were 2.4% (95% CI; -0.9-5.7) in AMB, and 2.4% (95% CI; -0.6-5.3) in PLB. The coronal
111 alignment difference between plane A and B was $16.8 \pm 2.2^\circ$ (range, 13.7-21.3), and plane B was more
112 valgus than plane A (**Figure 5**). On plane A, the diameters of the tunnel apertures were 7.0 ± 0.6 mm and
113 6.2 ± 0.6 mm in AMB, and 6.0 ± 0.4 mm and 5.3 ± 0.5 mm in PLB (major and minor axes, respectively).

114 On plane B, the diameters of the tunnel apertures were 7.0 ± 0.6 mm and 6.1 ± 0.5 mm in AMB, and 5.9
115 ± 0.4 mm and 5.3 ± 0.5 mm in PLB. No significant differences were observed in tunnel diameters between
116 the two planes (AMB major axis, $P = 0.28$; AMB minor axis, $P = 0.19$; PLB major axis, $P = 0.18$; PLB
117 minor axis, $P = 0.25$).

118

119 4. Discussion

120 The most important finding of this study was that the evaluation of tibial tunnel locations was not
121 significantly influenced by the selected plane in the AP direction. Moreover, although statistically
122 significant differences were found in ML direction, the differences in tunnel locations in ML direction
123 was subtle (only a couple of percentages); thus, these differences would not be clinically significant. These
124 findings suggest that both plane A and B can be used in the assessment of tibial tunnel location, and one
125 could assume that the results of the tibial tunnel locations may be compared and discussed using the grid
126 method among different institutions and different studies, as long as the grid is created consistently
127 between the studies. In our opinion, using plane A may be better for assessing the tibial tunnel locations
128 because plane A, which is parallel to the tibial plateau surface, would be clinically more straightforward
129 and the tibial shaft axis is not necessary to determine the plane. This consideration seems to be supported
130 by previous studies using the plane of tibial plateau surfaces[7,15].

131 In the ML direction, AMB and PLB tunnel apertures were significantly more laterally located in plane
132 A than plane B in the present study. Besides that, plane B was consistently located in more valgus than
133 plane A (**Figure 5**). This coronal plane difference could be because of the morphology of the proximal
134 tibia; the proximal tibia is physiologically varus, and medial proximal tibial angle has been reported to be
135 87° on average[22–24]. Thus, plane B, which is perpendicular to the tibial shaft axis, can be more valgus
136 than plane A, which is parallel to the tibial plateau joint surface. Moreover, tibial tunnels ran in antero-
137 medial direction from the aperture to the exit. Taken together, one could assume that the tunnel location

138 differences in ML direction could be at least partially attributable to this coronal alignment difference
139 between plane A and B.

140 Originally, tibial tunnel positions have been assessed using lateral plain radiographs of the knee[7,25].
141 The method, which was proposed by Amis et al., used the line parallel to the tibial articular surface[7] as
142 a reference, while Staubli et al. reported the use of a line perpendicular to the tibial bone axis[25] as a
143 reference. The limitation of assessment using plain lateral radiographs is that only AP direction can be
144 evaluated, and the rotation of the tibia might affect the results.

145 In recent years, a grid method using 3D bone models have been used to evaluate the tibial tunnel
146 locations after ACL reconstruction[11,12,14,26,27] (**Table 1**). This grid method with the top view of
147 proximal tibia has been also used for cadaveric studies to evaluate the location of the native ACL
148 insertions[11,13,14,28–30]. A recent MRI-based 3D topographic analysis[30] reported similar locations
149 of native AMB and PLB with these previous studies using 3D CT. A recent systematic review has reported
150 that the weighted mean of the center of native tibial AMB and PLB in 300 knees was 34.7% (the 5th and
151 95th percentiles; 25.0 and 41.0) and 47.8% (42.8 and 52.0) in AP direction[29], respectively. According
152 to this systematic review, the tibial tunnel locations in the present study were within the anatomical range
153 in the AP direction.

154 Lertwanich et al.[31] reported high intraobserver and interobserver reliability on the measurement of
155 ACL tunnel locations using 3D reconstructed models. However, these measurements may differ
156 depending on the process of 3D model preparation. Moon et al.[32] has shown that the rotation of the
157 proximal tibia significantly affected the measurement of tibial tunnel location using single-bundle ACL
158 reconstruction, and that the results of tibial tunnel locations significantly shifted to only medial direction
159 but not AP direction when the proximal tibia was rotated in valgus direction. Although they found
160 statistically significant differences, the translation of the tibial tunnel location was within only 3
161 percentages, thus the differences would not be clinically significant. This study by Moon et al. supports
162 the present results with double-bundle ACL reconstruction.

163 Several limitations of the present study should be mentioned. First, the present study assessed the
164 tunnel locations in double-bundle ACL reconstruction, but not single-bundle procedure. Nevertheless, we
165 believe that the current results can be transferred to single-bundle ACL reconstruction. Second, only
166 proximal tibial shaft was used to determine the tibial shaft axis. Ideally, the entire tibia would have been
167 needed to determine the accurate tibial shaft axis. But in consideration of radiation exposure, we did not
168 scan the entire tibia. However, we think it would be acceptable to determine the tibial shaft axis by using
169 the proximal tibia.

170

171 **5. Conclusion**

172 Although the tibial tunnel locations were not significantly influenced by the selected planes in the AP
173 direction, subtle but statistically significant differences were found in the ML direction between the plane
174 A (parallel to tibial plateau surfaces) and plane B (perpendicular to proximal tibial shaft axis) in double-
175 bundle ACL reconstruction. The findings suggest that both plane A and B can be used in the assessment
176 of tibial tunnel locations after ACL reconstruction.

177

178 **Declaration of competing interest**

179 This research did not receive any specific grant from funding agencies in the public, commercial, or not-
180 for-profit sectors.

181

182 **Acknowledgements**

183 Providing language help was performed by professional editors at Editage, a division of Cactus
184 Communications.

- 186 [1] Rodríguez-Merchán EC, Durán D, Revilla C, Gómez-Cardero P, Martínez-Lloreda Á, Bello S.
187 Arthroscopic BPTB graft reconstruction in ACL ruptures: 15-year results and survival. *Knee*
188 2014;21:902–5. doi:10.1016/j.knee.2014.07.004.
- 189 [2] Rodríguez-Merchan EC. Evidence-based ACL reconstruction. *Arch Bone Jt Surg* 2015;3:9–12.
190 doi:10.22038/abjs.2015.3769.
- 191 [3] Khalfayan EE, Sharkey PF, Alexander AH, Bruckner JD, Bynum EB. The relationship between
192 tunnel placement and clinical results after anterior cruciate ligament reconstruction. *Am J Sports*
193 *Med* 1996;24:335–41. doi:10.1177/036354659602400315.
- 194 [4] Rayan F. Review of evolution of tunnel position in anterior cruciate ligament reconstruction.
195 *World J Orthop* 2015;6:252. doi:10.5312/wjo.v6.i2.252.
- 196 [5] Ohsawa T, Kimura M, Hagiwara K, Yorifuji H, Takagishi K. Clinical and second-look
197 arthroscopic study comparing 2 tibial landmarks for tunnel insertions during double-bundle acl
198 reconstruction with a minimum 2-year follow-up. *Am J Sports Med* 2012;40:2479–86.
199 doi:10.1177/0363546512458257.
- 200 [6] Hatayama K, Terauchi M, Saito K, Higuchi H, Yanagisawa S, Takagishi K. The importance of
201 tibial tunnel placement in anatomic double-bundle anterior cruciate ligament reconstruction.
202 *Arthroscopy* 2013;29:1072–8. doi:10.1016/j.arthro.2013.02.003.
- 203 [7] Amis AA, Jakob RP. Anterior cruciate ligament graft positioning, tensioning and twisting. *Knee*
204 *Surg Sport Traumatol Arthrosc* 1998;6:S2–12. doi:10.1007/s001670050215.
- 205 [8] Kasten P, Szczodry M, Irrgang J, Kropf E, Costello J, Fu FH. What is the role of intra-operative
206 fluoroscopic measurements to determine tibial tunnel placement in anatomical anterior cruciate

207 ligament reconstruction? *Knee Surg Sport Traumatol Arthrosc* 2010;18:1169–75.
 208 doi:10.1007/s00167-010-1082-8.

209 [9] Doi M, Takahashi M, Abe M, Suzuki D, Nagano A. Lateral radiographic study of the tibial sagittal
 210 insertions of the anteromedial and posterolateral bundles of human anterior cruciate ligament.
 211 *Knee Surg Sport Traumatol Arthrosc* 2009;17:347–51. doi:10.1007/s00167-008-0668-x.

212 [10] Staubli HU, Rauschning W. Tibial attachment area of the anterior cruciate ligament in the
 213 extended knee position. Anatomy and cryosections in vitro complemented by magnetic resonance
 214 arthrography in vivo. *Knee Surg Sports Traumatol Arthrosc* 1994;2:138–46.

215 [11] Lorenz S, Elser F, Mitterer M, Obst T, Imhoff AB. Radiologic evaluation of the insertion sites of
 216 the 2 functional bundles of the anterior cruciate ligament using 3-dimensional computed
 217 tomography. *Am J Sports Med* 2009;37:2368–76. doi:10.1177/0363546509341577.

218 [12] Forsythe B, Kopf S, Wong AK, Martins CAQ, Anderst W, Tashman S, et al. The location of
 219 femoral and tibial tunnels in anatomic double-bundle anterior cruciate ligament reconstruction
 220 analyzed by three-dimensional computed tomography models. *J Bone Jt Surg - Ser A*
 221 2010;92:1418–26. doi:10.2106/JBJS.I.00654.

222 [13] Abreu-e-Silva GM de, Oliveira MHGCN de, Maranhão GS, Deligne L de MC, Pfeilsticker RM,
 223 Novais ENV, et al. Three-dimensional computed tomography evaluation of anterior cruciate
 224 ligament footprint for anatomic single-bundle reconstruction. *Knee Surg Sport Traumatol*
 225 *Arthrosc* 2015;23:770–6. doi:10.1007/s00167-013-2703-9.

226 [14] Lee JK, Lee S, Seong SC, Lee MC. Anatomy of the anterior cruciate ligament insertion sites:
 227 comparison of plain radiography and three-dimensional computed tomographic imaging to
 228 anatomic dissection. *Knee Surg Sport Traumatol Arthrosc* 2015;23:2297–305.
 229 doi:10.1007/s00167-014-3041-2.

- 230 [15] Parkinson B, Gogna R, Robb C, Thompson P, Spalding T. Anatomic ACL reconstruction: the
231 normal central tibial footprint position and a standardised technique for measuring tibial tunnel
232 location on 3D CT. *Knee Surg Sport Traumatol Arthrosc* 2017;25:1568–75. doi:10.1007/s00167-
233 015-3683-8.
- 234 [16] Lee DW, Kim JG, Lee JH, Park JH, Kim DH. Comparison of Modified Transtibial and Outside-In
235 Techniques in Anatomic Single-Bundle Anterior Cruciate Ligament Reconstruction. *Arthroscopy*
236 2018;34:2857–70. doi:10.1016/j.arthro.2018.05.041.
- 237 [17] Chiba D, Yamamoto Y, Kimura Y, Sasaki S, Tsuda E, Ishibashi Y. Combination of anterior tibial
238 and femoral tunnels makes the signal intensity of antero-medial graft higher in double-bundle
239 anterior cruciate ligament reconstruction. *Knee Surg Sport Traumatol Arthrosc* 2020 in press
240 doi:10.1007/s00167-020-06014-4.
- 241 [18] Miyaji N, Araki D, Hoshino Y, Kanzaki N, Nagai K, Matsumoto T, et al. The sagittal cutting
242 plane affects evaluation of the femoral bone tunnel position on three-dimensional computed
243 tomography after anterior cruciate ligament reconstruction. *Knee Surg Sport Traumatol Arthrosc*
244 2020 in press doi:10.1007/s00167-020-05963-0.
- 245 [19] Araki D, Kuroda R, Kubo S, Fujita N, Tei K, Nishimoto K, et al. A prospective randomised study
246 of anatomical single-bundle versus double-bundle anterior cruciate ligament reconstruction:
247 quantitative evaluation using an electromagnetic measurement system. *Int Orthop* 2011;35:439–
248 46. doi:10.1007/s00264-010-1110-9.
- 249 [20] Matsushita T, Nagai K, Araki D, Tanaka T, Matsumoto T, Nishida K, et al. Factors associated
250 with the status of meniscal tears following meniscal repair concomitant with anterior cruciate
251 ligament reconstruction. *Connect Tissue Res* 2017;58:386–92.
252 doi:10.1080/03008207.2017.1281257.

- 253 [21] Nagai K, Tashiro Y, Herbst E, Gale T, Wang JH, Irrgang JJ, et al. Steeper posterior tibial slope
254 correlates with greater tibial tunnel widening after anterior cruciate ligament reconstruction. *Knee*
255 *Surg Sport Traumatol Arthrosc* 2018;26:3717–23. doi:10.1007/s00167-018-5004-5.
- 256 [22] Colyn W, Agricola R, Arnout N, Verhaar JAN. How does lower leg alignment differ between
257 soccer players , other athletes , and non - athletic controls ? *Knee Surg Sport Traumatol Arthrosc*
258 2016;24:3619–26. doi:10.1007/s00167-016-4348-y.
- 259 [23] Thienpont E, Schwab PE, Cornu O, Bellemans J, Victor J. Bone morphotypes of the varus and
260 valgus knee. *Arch Orthop Trauma Surg* 2017;137:393–400. doi:10.1007/s00402-017-2626-x.
- 261 [24] Degen N, Sass J, Jalali J, Kovacs L, Euler E, Prall WC, et al. Three-dimensional assessment of
262 lower limb alignment: Reference values and sex-related differences. *Knee* 2020;27:428–35.
263 doi:10.1016/j.knee.2019.11.009.
- 264 [25] Stäubli HU, Rauschning W. Tibial attachment area of the anterior cruciate ligament in the
265 extended knee position - Anatomy and cryosections in vitro complemented by magnetic
266 resonance arthrography in vivo. *Knee Surg Sport Traumatol Arthrosc* 1994;2:138–46.
267 doi:10.1007/BF01467915.
- 268 [26] Ohori T, Mae T, Shino K, Tachibana Y, Sugamoto K, Yoshikawa H, et al. Morphological
269 changes in tibial tunnels after anatomic anterior cruciate ligament reconstruction with hamstring
270 tendon graft. *J Exp Orthop* 2017;4. doi:10.1186/s40634-017-0104-6.
- 271 [27] Taketomi S, Inui H, Yamagami R, Shirakawa N, Kawaguchi K, Nakagawa T, et al. Bone-Patellar
272 Tendon-Bone Autograft versus Hamstring Tendon Autograft for Anatomical Anterior Cruciate
273 Ligament Reconstruction with Three-Dimensional Validation of Femoral and Tibial Tunnel
274 Positions. *J Knee Surg* 2018;31:866–74. doi:10.1055/s-0037-1615813.

- 275 [28] Hoogeslag RAG, Brouwer RW, Huis in 't Veld R, Amis AA. Isometric placement of the
276 augmentation braid is not attained reliably in contemporary ACL suture repair. *Knee*
277 2020;27:111–23. doi:10.1016/j.knee.2019.10.013.
- 278 [29] Parkar AP, Adriaensen MEAPM, Vindfeld S, Solheim E. The Anatomic Centers of the Femoral
279 and Tibial Insertions of the Anterior Cruciate Ligament: A Systematic Review of Imaging and
280 Cadaveric Studies Reporting Normal Center Locations. *Am J Sports Med* 2017;45:2180–8.
281 doi:10.1177/0363546516673984.
- 282 [30] Dimitriou D, Wang Z, Zou D, Helmy N, Tsai TY. Do Sex-Specific Differences Exist in ACL
283 Attachment Location? An MRI-Based 3-Dimensional Topographic Analysis. *Orthop J Sport Med*
284 2020;8:1–7. doi:10.1177/2325967120964477.
- 285 [31] Lertwanich P, Martins CAQ, Asai S, Ingham SJM, Smolinski P, Fu FH. Anterior cruciate
286 ligament tunnel position measurement reliability on 3-dimensional reconstructed computed
287 tomography. *Arthroscopy* 2011;27:391–8. doi:10.1016/j.arthro.2010.08.018.
- 288 [32] Moon HS, Choi CH, Jung M, Lee DY, Chang H, Kim SH. Do Rotation and Measurement
289 Methods Affect Reliability of Anterior Cruciate Ligament Tunnel Position on 3D Reconstructed
290 Computed Tomography? *Orthop J Sport Med* 2019;7:1–11. doi:10.1177/2325967119885882.

Figure Legends

Figure 1. Description of the plane A which was parallel to tibial plateau.

Medial and lateral articular surfaces of the tibial plateau were selected (green) and then the plane A (blue grid), which is parallel to the selected areas, was obtained.

Figure 2. Description of the plane B which was perpendicular to tibial shaft axis.

(a) proximal tibial shaft was selected (green) and the axis of selected area (red line) is automatically created.

(b) the plane B (blue grid), which was perpendicular to proximal tibial shaft axis was created. In proximal-distal direction, the plane B was put beneath the aperture where a complete ellipse could be drawn around the tunnels.

Figure 3. The measurement of tibial tunnel aperture locations using a grid method.

Anterior-posterior and medial-lateral axes were established, and the location of tunnel apertures were expressed as a percentage of the corresponding maximum dimension.

Figure 4. Scatter plots of the tibial tunnel locations using two planes.

(a) Locations of anteromedial bundle (AMB) (b) Locations of posterolateral bundle (PLB)

Figure 5. Coronal alignment difference between plane A and plane B.

An example shows the difference in coronal alignment between plane A and plane B, and the plane B was more valgus than plane A.

318

323

325

326
327

328
329
330

331
332
333
334
335

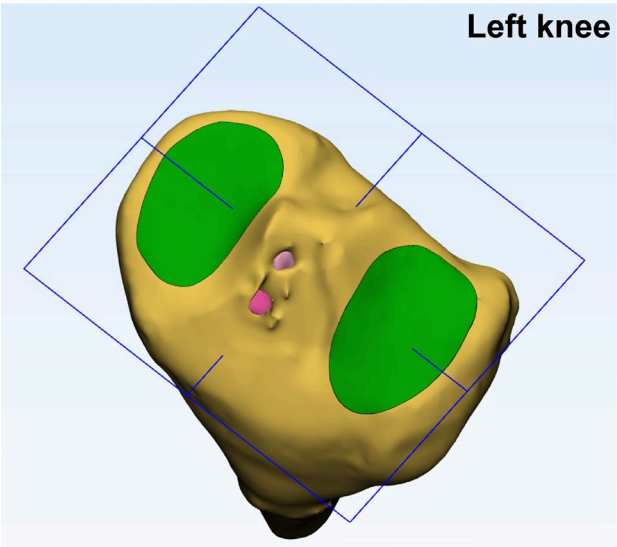


Figure 1.

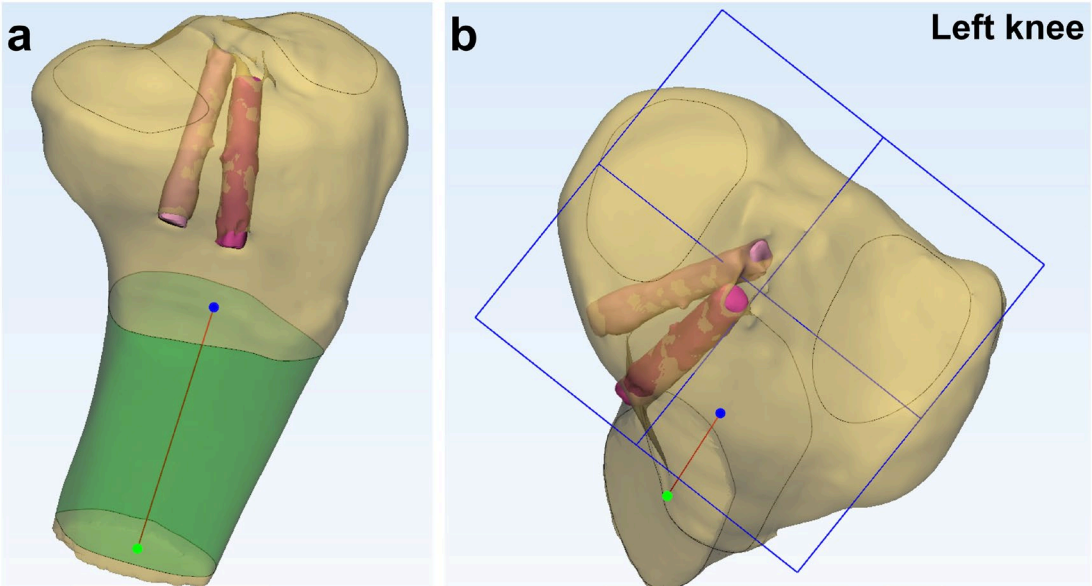


Figure 2.

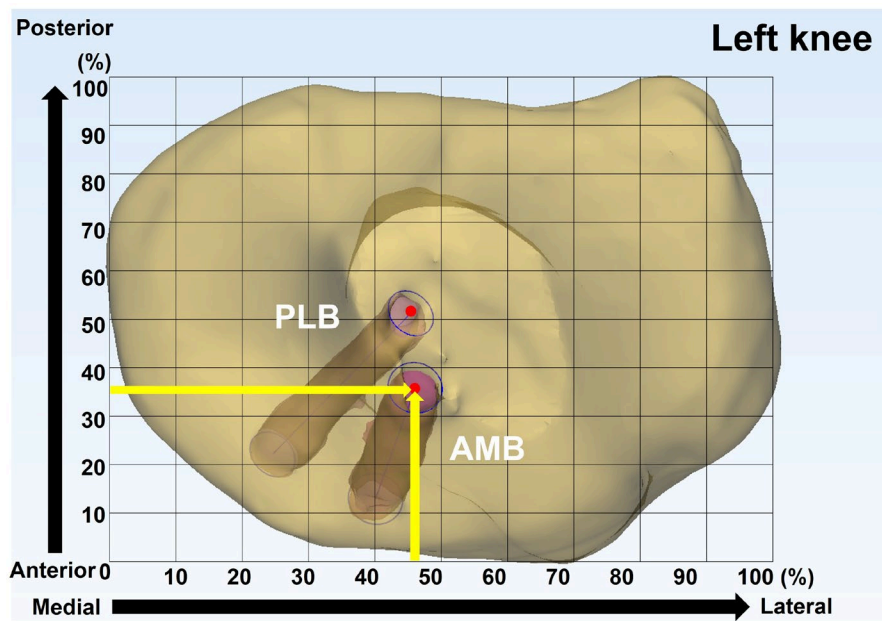


Figure 3.

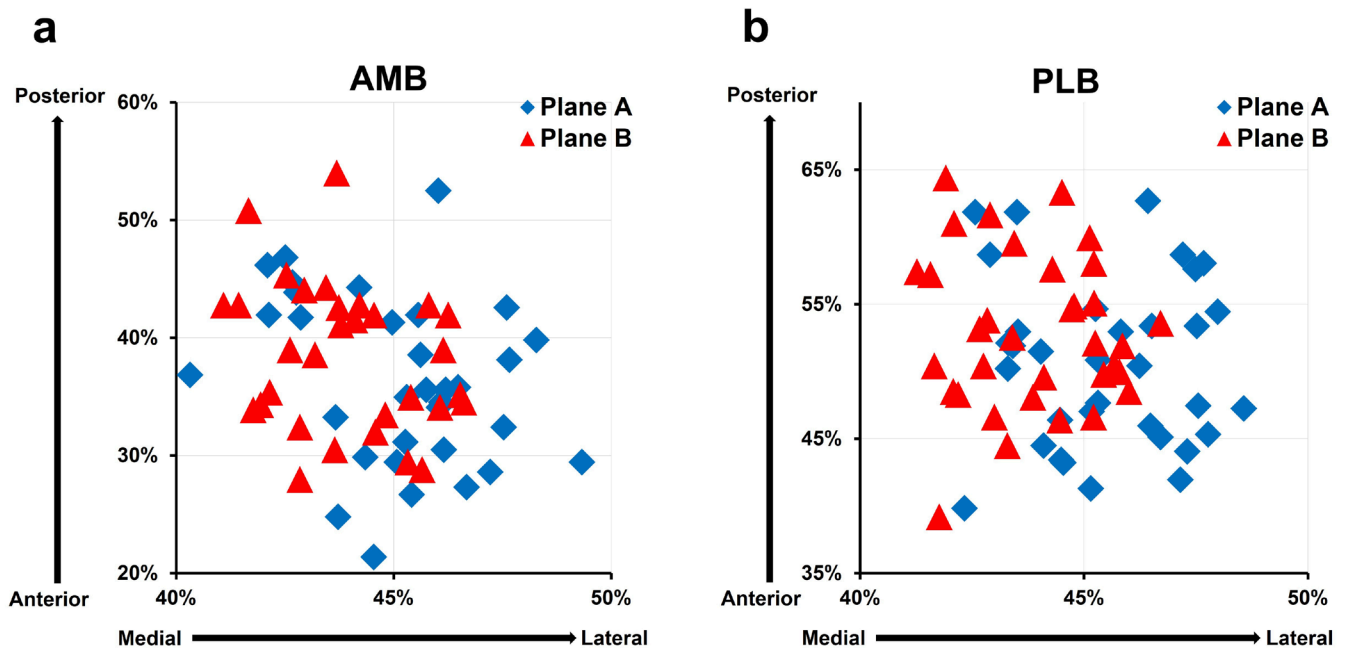
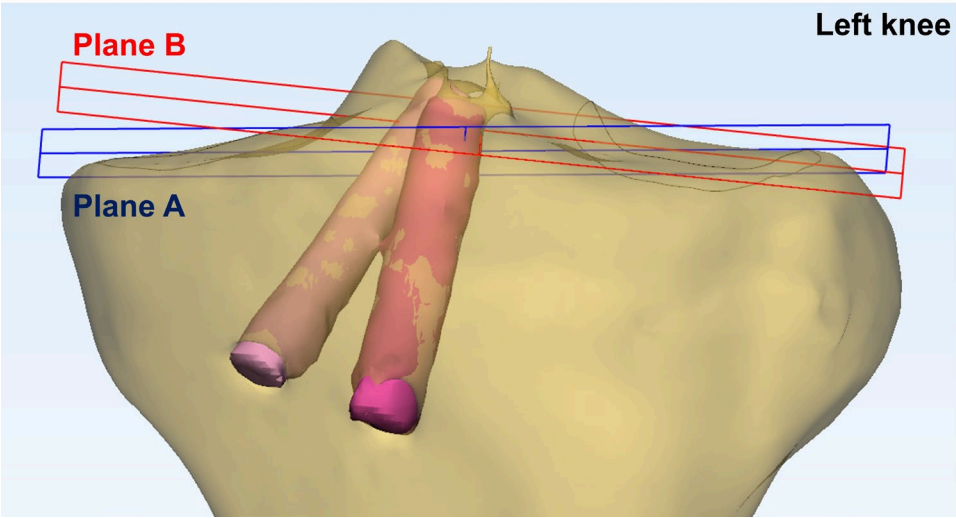


Figure 4.

344

345



346

347 Figure 5.